Computational Geosciences **5:** 47–60, 2001.

Multi-scale and multi-resolution stochastic modeling of subsurface heterogeneity by tree-indexed Markov chains

Michel Dekking [a], Amro Elfeki [b], Cor Kraaikamp [a] and Johannes Bruining [c]

[a] *Thomas Stieltjes Institute of Mathematics and Delft University of Technology, Faculty ITS, Department CROSS, P.O. Box 5031, 2600 GA Delft, The Netherlands*
E-mail: F.M.Dekking@math.tudelft.nl
[b] *Mansoura University, Department of Civil Engineering, Faculty of Engineering, Mansoura, Egypt*
[c] *Delft University of Technology, Faculty of Applied Earth Sciences, Mijnbouwstraat 120, 2628 RX Delft, The Netherlands*

Accepted 19 June 2001

A new methodology is proposed to handle multi-scale heterogeneous structures. It can be of importance in the field of hydrogeology and for petroleum engineers who are interested in characterizing subsurface heterogeneity at various scales. The framework of this methodology is based on a coarse to fine scale representation of the heterogeneous structures on trees. Different depths in the tree correspond to different spatial scales in representing the heterogeneous structures on trees. On these trees a Markov chain is used to describe scale to scale transitions and to account for the uncertainty in the stochastically generated images.

We focus in this work on the description and application of the methodology to synthetic data that are geologically realistic. The methodology is flexible. Conditioning on field data and measurements is straightforward. Non-stationary and stationary fields, compound and nested structures can be addressed.

Keywords: multi-scales, stochastic modeling, heterogeneity, tree-indexed Markov chains, subsurface characterization

1. Introduction

Characterization of the subsurface that incorporates the dominant features of the geological heterogeneity at the significant scales of variability is essential in the field of groundwater hydrology for predicting the spreading of contaminants. It is also of great importance to petroleum engineers to improve oil recovery. Extensive studies have been devoted to mono-scale heterogeneous structures based on the theory of stationary random fields [16]. Reviews of these methods are presented in the literature of hydrogeology (see, e.g., [13]) and in the literature of petroleum engineering (e.g., [4,11,18]).

It has also been proposed to apply the concept of fractals to model phenomena which possess self-similarity over all scales (see, e.g., [1;18, chapter 19]). However, in real formations one often encounters different geometrical shapes with different

anisotropy structure at each scale (e.g., a sedimentological bedform such as small-scale laminations, cross-beddings, ripples and dunes embedded in a large-scale stratigraphic architecture). Examples of this type of heterogeneity are presented in many outcrops (see, e.g., [15]). Some studies tried to handle this type of heterogeneity using a hybrid approach (see, e.g., [11]). In this approach, the discrete geological attributes (facies) are modeled using indicator geostatistics, while the microstructures are treated in a continuous sense within the individual facies using Gaussian random fields. This hybrid approach has been adopted by many authors (see, e.g., [6]). It enables one to characterize variability at two different scales, the so-called macro- and mega-scales [17]. It has been applied to study the influence of geological and parametric uncertainty on solute transport predictions [10].

The motivation of the current research stems from the fact that natural formations exhibit different geometrical shapes at a multiplicity of scales with different structural anisotropy patterns at each scale. To the best of the authors' knowledge, there is no systematic methodology that can characterize this type of multi-scale heterogeneous structure with different geometrical patterns and bedding type at each scale. The framework of the methodology described in this paper is based on a coarse to fine scale representation of the heterogeneous structures on trees. Different depths in the tree correspond to different spatial scales in representing the heterogeneous structures. On these trees, an inhomogeneous Markov chain is used to describe scale to scale transitions and to account for uncertainty in the heterogeneous system over all scales. Such a framework provides the link between the geological description of the reservoir and the hydrodynamic model of interest to a reservoir engineer. This link will be considered in future work. The work presented here describes the proposed methodology and demonstrates some of its applications on synthetic data.

2. Basic definitions and terminology

2.1. Quad trees

Quad trees are hierarchical data structures used to represent spatial data or images. They are based on the principle of recursive decomposition of an image into its corresponding scales. Each level in the hierarchical structure corresponds to a particular spatial scale and each node at a given scale is connected to a node at the next coarser scale and to several descendent nodes at the next finer scale. This type of representation is commonly used (see, e.g., [14]). A 2-dimensional image with $2^K \times 2^K$ pixels consists in a natural way of K scales (levels). At a particular scale or level L_M, where $0 \leqslant M \leqslant K$, the corresponding number of grid cells at this scale is $2^M \times 2^M$. There is a factor 4 between the number of grid cells at each scale and the previous coarser one. This yields the quad tree structure over all scales of an image. The procedure is simply based on the successive subdivision of an image into four equal sized quadrants. In case of binary images, which contain only black (B) or white (W) pixels, if the image does not consist entirely of blacks or entirely of whites, it is declared gray (G) and is

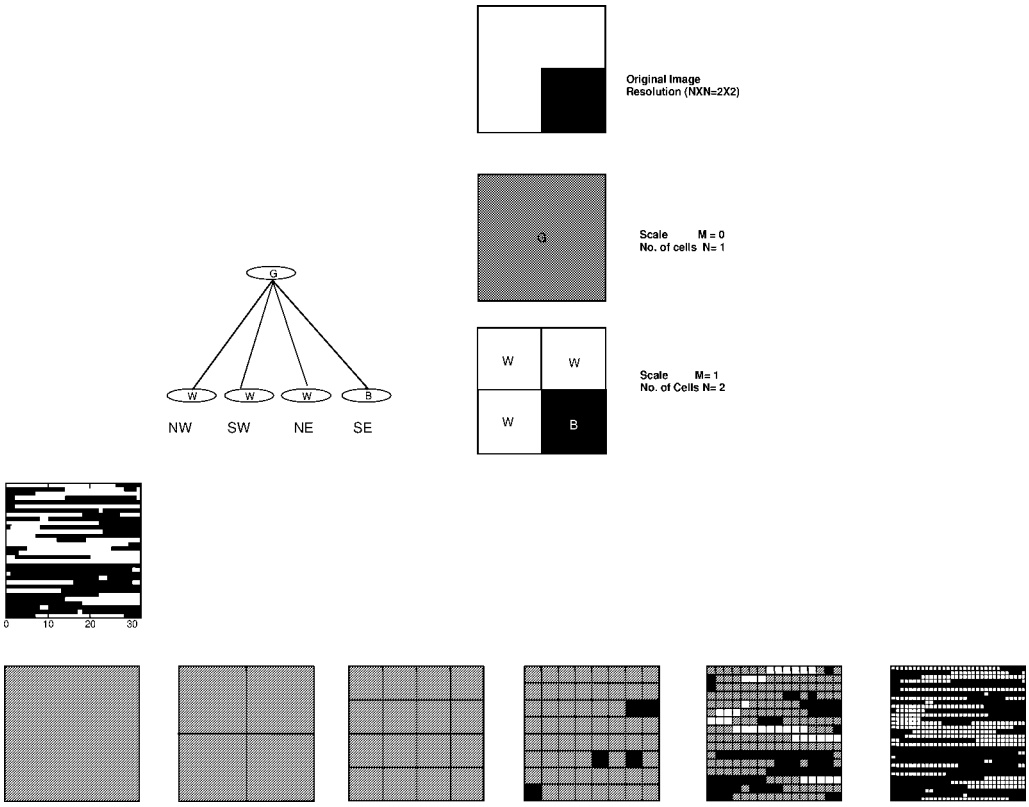

Figure 1. Quad tree representation of an image: the top illustrates the tree description of an image; the bottom shows the scale resolution of an image with 32×32 pixels (scales $M = 0, 1, 2, 3, 4$ and 5, respectively, from left to right).

subdivided into quadrants, subquadrants, and so on, until blocks are obtained that consist entirely of blacks or whites. The idea of using quad tree representations of binary images has been used earlier in [3] to characterize lung scan images. Figure 1 illustrates the method.

In general, a tree is a connected graph without loops or cycles and with a distinguished vertex that precedes all other nodes in the tree and which is called the "root". It is denoted by the symbol Λ, and corresponds to level $M = 0$. In general, a node with its four descendents is called the "father", respectively the "children". Each child represents a quadrant (labeled in order NW, SW, NE, SE) of the region represented by that node.

2.2. *Tree-indexed Markov chains*

Images can be randomized by randomly labeling the corresponding quad trees. A natural way to accomplish this is by using a Markov chain. A Markov chain on the

tree describes a scale-to-scale transition. Formally this should be called a tree-indexed Markov chain. For vertices u and v on the tree, one can write $u \leqslant v$ if u is on the unique path from v to the root Λ.

The set of vertices of the tree will be denoted by T. For any vertex w in T which is not the root Λ, we denote the father of w by $\overleftarrow{w}$, i.e., the unique vertex connected to w with $\overleftarrow{w} \leqslant w$. For any $v \in T$ we let $T(v)$ be the subtree of T with v as its root, i.e., $T(v) = \{w \in T\colon\ v \leqslant w\}$. A tree-indexed Markov chain (indexed by a tree T) is a collection $\{X_w\colon\ w \in T\}$ of random variables taking values in a finite set $\mathcal{S}$ of states, satisfying the (tree) Markovian property, i.e., for each $w \in T$, $w \neq \Lambda$,

$$P(X_w = \beta \mid X_{\overleftarrow{w}} = \alpha,\ X_{T\setminus T(w)}) = P(X_w = \beta \mid X_{\overleftarrow{w}} = \alpha), \quad \alpha, \beta \in \mathcal{S}.$$

Here we denote $X_U = \{X_u\colon\ u \in U\}$ for a subset U of T. Let $w \in T$, $w \neq \Lambda$, and let $v = \overleftarrow{w}$. We call

$$p_\Lambda(\alpha) = P(X_\Lambda = \alpha) \quad \text{and} \quad p_{v,w}(\alpha, \beta) = P(X_w = \beta \mid X_v = \alpha), \quad \alpha, \beta \in \mathcal{S},$$

the initial distribution and the transition probabilities of the chain.

2.3. *Tree-indexed Markov chains on quad trees*

For a tree-indexed Markov chain X_T, and for $v \in T$, the marginal probability $P(X_v = \alpha)$ can be expressed in the initial distribution and the transition probabilities, proceeding just as in the case of ordinary Markov chains. To be more precise, if we denote

$$p_v(\alpha) = P(X_v = \alpha), \quad v \in T,$$

and if U is a finite connected subset of T, then Dekking et al. obtained in [3] the following result.

Theorem 1. Let $\Lambda(U)$ denote the unique vertex in U with $\Lambda(U) \leqslant v$ for all $v \in U$. Then

$$P(X_V = \beta_V) = p_{\Lambda(V)}(\beta_{\Lambda(V)}) \cdot \prod_{v \in V, v \neq \Lambda(V)} p_{\overleftarrow{v},v}(\beta_{\overleftarrow{v}}, \beta_v).$$

For an arbitrary tree T we define its levels $L_M = L_M(T)$, by $L_0 = \Lambda$ and $L_{M+1} = \{w \in T\colon\ \overleftarrow{w} \in L_M\}$ for $M = 0, 1, 2, \ldots, K$. If $w \in L_M$ we write $\mathrm{Lev}(w) = M$. With an image consisting of $2^K \times 2^K$ pixels we associate the 4-ary tree T_K^4, i.e., all level K vertices are leaves, and for each v with $\mathrm{Lev}(v) < K$ one has $\#\{w\colon\ \overleftarrow{w} = v\} = 4$ (see figure 1). To randomize the quad tree of an image consisting of $2^K \times 2^K$ pixels in a T_K^4-indexed Markov chain we already saw that we should have as state space $\mathcal{S} = \{B, W, G\}$ representing the colors white, black and gray. Furthermore, it is required that $p_{v,w}(W, W) = p_{v,w}(B, B) = 1$, for all $v,w \in T_K^4$, such that $v = \overleftarrow{w}$. This corresponds to the fact that the algorithm stops when the pixels in a subsquare are either all white or all

black. With this definition the tree itself is not image dependent: the randomness resides in the transitions from G to B, W and G.

Although the whole idea of a tree-indexed Markov chain on a quad tree is conceptually simple some care has to be taken. It turns out that it is only possible to define quite restricted T_K^4-indexed Markov chains. Let w_1, w_2, w_3 and w_4 be four vertices having the same father v, i.e., $\overleftarrow{w}_i = v$ for $i = 1, 2, 3$ and 4. Then

$$P(X_{w_1} = W \mid X_v = G,\ X_{w_2} = W,\ X_{w_3} = W,\ X_{w_4} = W) = 0$$

but by the Markov property this probability should be equal to

$$P(X_{w_1} = W \mid X_v = G),$$

which, in general, will be positive. In other words, in this model (the so called 1–1 model) non-admissible sequences can be generated with positive probability. I.e., it is possible that a "gray" father has four children of the same color (different from "gray"), which is in violation with the definition of the father being in a state labeled "gray". The way out of this problem is to interpret quadruples of vertices having the same father as a single vertex. This gives a T_{K-1}^4-indexed Markov chain with state space $\mathcal{S}^4 = \{B, W, G\}^4$ and transition probabilities

$$p_{\underline{v},\underline{w}}(\underline{\alpha}, \underline{\beta}) = p_{(v_1,v_2,v_3,v_4),(w_1,w_2,w_3,w_4)}\big((\alpha_1, \alpha_2, \alpha_3, \alpha_4), (\beta_1, \beta_2, \beta_3, \beta_4)\big) \tag{1}$$

$\alpha_i, \beta_j \in \Gamma$, with $\overleftarrow{w}_j = v_i$ for some i and $\overleftarrow{v}_1 = \overleftarrow{v}_2 = \overleftarrow{v}_3 = \overleftarrow{v}_4$. This model is also known as the 4–4 model. Other variations from the so-called 1–1 model will be discussed in the next sections.

2.4. Estimation of transition probabilities from data

In this section we show how to obtain the parameters of the model from data. Suppose there are M_{tot} images with corresponding trees, i.e., these trees are realizations of a tree-indexed Markov chain X_T with transition probabilities $p_{v,w}(\alpha, \beta)$ for $w \in T$ and $\alpha, \beta \in \mathcal{S}$. Here it is always assumed that $v = \overleftarrow{w}$. Let $w \in T$ and $1 \leqslant m \leqslant M_{\text{tot}}$ the color of vertex w in the mth data tree be denoted by X_w^m. One can define for $\alpha, \beta \in \mathcal{S}$, $w \in T$

$$N_w(\alpha) = \#\big\{m:\ X_w^m = \alpha\big\}, \qquad N_{v,w}(\alpha, \beta) = \#\big\{m:\ X_v^m = \alpha,\ X_w^m = \beta\big\}.$$

Furthermore, one can define the empirical transition probabilities

$$\hat{p}_{v,w}(\alpha, \beta) = \begin{cases} \dfrac{N_{v,w}(\alpha, \beta)}{N_v(\alpha)}, & \text{in case } N_v(\alpha) \neq 0, \\ 0, & \text{in case } N_v(\alpha) = 0, \end{cases}$$

and the initial empirical probabilities by

$$\hat{p}_\Lambda(\alpha) = \frac{N_\Lambda(\alpha)}{M_{\text{tot}}}.$$

In [3] it was shown that these empirical transition probabilities $\hat{p}_{v,w}(\alpha, \beta)$ and initial probabilities $\hat{p}_\Lambda(\alpha)$ are in some sense the "right" estimators for the probabilities $p_{v,w}(\alpha, \beta)$ and $p_\Lambda(\alpha)$, respectively.

Theorem 2. The empirical transition and initial probabilities are the maximum likelihood estimators for $p_{v,w}(\alpha, \beta)$ and $p_\Lambda(\alpha)$, respectively.

For a *proof*, see [3].

Since $\hat{p}_\Lambda(\alpha) = N_\Lambda(\alpha)/M_{\text{tot}}$, it at once follows from the fact that $N_\Lambda(\alpha)$ is a binomial random variable with parameters M_{tot} and $\hat{p}_\Lambda(\alpha)$ that $E\,\hat{p}_\Lambda(\alpha) = p_\Lambda(\alpha)$, i.e., $\hat{p}_\Lambda(\alpha)$ is an unbiased estimator for $p_\Lambda(\alpha)$. Surprisingly, the empirical transition probability $\hat{p}_{v,w}(\alpha, \beta)$ is a biased estimator for $p_{v,w}(\alpha, \beta)$. We have the following proposition.

Proposition 3. Setting $q_v = 1 - p_v(\alpha)$, one has that

$$E\,\hat{p}_{v,w}(\alpha, \beta) = p_{v,w}(\alpha, \beta)\big[1 - q_v^{M_{\text{tot}}}\big].$$

Proof. Taking conditional expectation, and recalling that $\hat{p}_{v,w}(\alpha, \beta) = 0$ in case $N_v(\alpha) = 0$ and $\hat{p}_{v,w}(\alpha, \beta) = N_{v,w}(\alpha, \beta)/N_v(\alpha)$ in case $N_v(\alpha) \neq 0$, one has

$$\begin{aligned} E\,\hat{p}_{v,w}(\alpha, \beta) &= E\,E\big\{\hat{p}_{v,w}(\alpha, \beta) \mid N_v(\alpha)\big\} \\ &= \sum_{n=0}^{\infty} E\big\{\hat{p}_{v,w}(\alpha, \beta) \mid N_v(\alpha) = n\big\} P\big(N_v(\alpha) = n\big) \\ &= \sum_{n=1}^{\infty} E\left\{\frac{N_{v,w}(\alpha, \beta)}{N_v(\alpha)} \mid N_v(\alpha) = n\right\} P\big(N_v(\alpha) = n\big). \end{aligned}$$

Conditional on the event $\{N_v(\alpha) = n\}$, where $n \geqslant 1$, $N_{v,w}(\alpha, \beta)$ is a binomial random variable with parameters n and $p_{v,w}(\alpha, \beta)$, and we find that

$$\begin{aligned} E\,\hat{p}_{v,w}(\alpha, \beta) &= \sum_{n=1}^{\infty} \frac{1}{n} n p_{v,w}(\alpha, \beta) P\big(N_v(\alpha) = n\big) \\ &= p_{v,w}(\alpha, \beta) P\big(N_v(\alpha) > 0\big). \end{aligned}$$

Since $q_v^{M_{\text{tot}}} = P(N_v(\alpha) = 0)$, the results follows. □

3. Geological applications

3.1. Synthetic data used in the simulations

To generate synthetic data for the tree-indexed Markov chain model we use the coupled Markov chain model developed in [9]. In this model two ordinary Markov chains are coupled. The first one is used to describe the sequence in lithology in the

vertical direction and the second chain describes the sequence of variation in the horizontal direction. The two chains are coupled in the sense that a state of a cell in the domain is dependent on the state of two cells, the one on top and the other on the left of the current cell. This dependence is described in terms of transition probabilities from the two chains. The coupled Markov chain technique is efficient in terms of computer time and storage in comparison with other techniques available in the literature such as sequential indicator simulation [4] and truncated Gaussian methods [11]. Although itself a Markov random field [7], it is also efficient when compared with general Markov random fields [2]. Some examples of input data that is generated by the coupled Markov chain model are shown in the following sections.

Figure 2 top row shows two images that are generated by the coupled Markov chain model. The input parameters (transition probabilities) for generating these images are presented in table 1. The geological system consists of two different lithologies that appear in black and white. Let (p_{ij}^{H}) be the transition probability matrix giving the probabilities p_{ij}^{H} that a lithology i is followed by lithology j. These are given in the left side of tables 1 and 2 (e.g., the probability that B is followed by B in the horizontal direction on the large scale is 0.98). A similar transition probability matrix (p_{ij}^{V}) is used in the vertical direction.

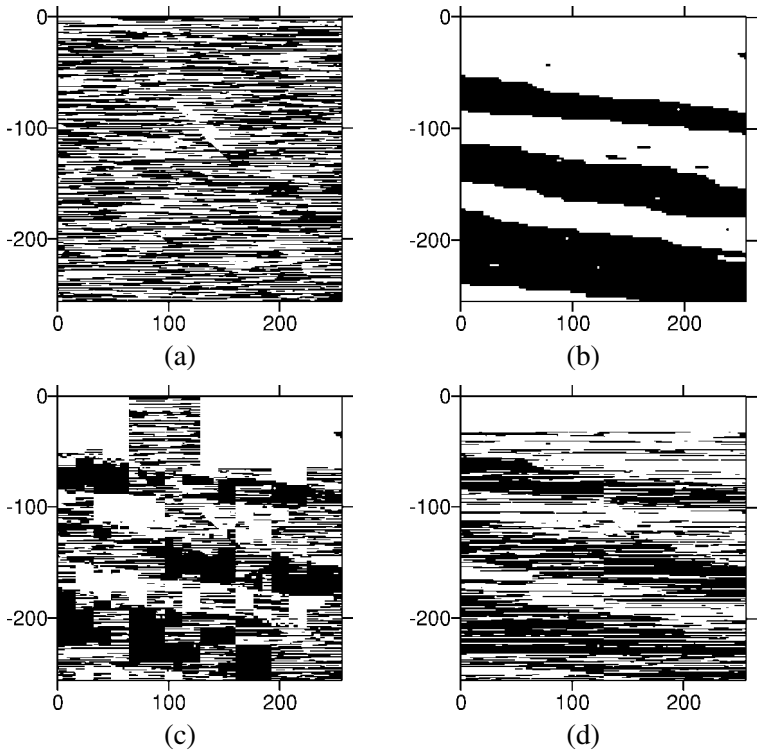

Figure 2. Merging two different heterogeneous structures by quad, respectively dyadic trees. (a), (b): input data; (c): simulation with the quad tree; (d): simulation with the dyadic tree (image resolution 256×256).

Table 1
Input parameters to generate the large-scale structure in figure 2(b).

Horizontal transition matrix			Vertical transition matrix		
State	B	W	State	B	W
B	0.98	0.02	B	0.80	0.20
W	0.02	0.98	W	0.20	0.80

Table 2
Input parameters to generate the fine-scale structure in figure 2(a).

Horizontal transition matrix			Vertical transition matrix		
State	B	W	State	B	W
B	0.97	0.03	B	0.50	0.50
W	0.03	0.97	W	0.50	0.50

3.2. Quad tree simulation example

In this example the merging of two structures is presented. A large-scale layered system (figure 2(b)) and micro-scale laminations (figure 2(a)) are considered. The simulations produce discontinuity at all scales (see figure 2(c)). These results are not satisfactory from a geological point of view, since many vertical discontinuities appear which are not present in the original image.

3.3. Dyadic trees

The example in the previous section shows that the quad tree method is not very suitable from a geological point of view. Natural geological deposits exhibit very long extensions comparable with their thickness. This is due to the sedimentary origin of these deposits. With this in mind, we switch from quad trees to so called *dyadic trees*. In the dyadic tree any node in the tree has two descendent nodes at the next finer scale and one parent node at the preceding coarser scale (see figure 3(a), the 1-2V 1-2H model).

Different levels in the tree correspond to different scales of the image. In particular, the 2^M values at the Mth level of the tree are interpreted as describing certain details about the Mth scale of the image that is not present at coarser resolution.

In 2-dimensional images dyadic trees are used in both vertical and horizontal directions respectively. Firstly, the image is decomposed into its corresponding scales in the vertical direction by a dyadic tree 2^{K_y} until the pixel level in the vertical direction is reached. Secondly, the features that do not appear in the vertical direction will appear when the scaling in the horizontal direction is performed. The strips that appeared in gray are then scaled horizontally by 2^{K_x} into their corresponding levels in the horizontal direction until the pixel level is reached in the horizontal direction. An image that is described by the dyadic tree is shown in figure 3(b). To introduce more correlation into the

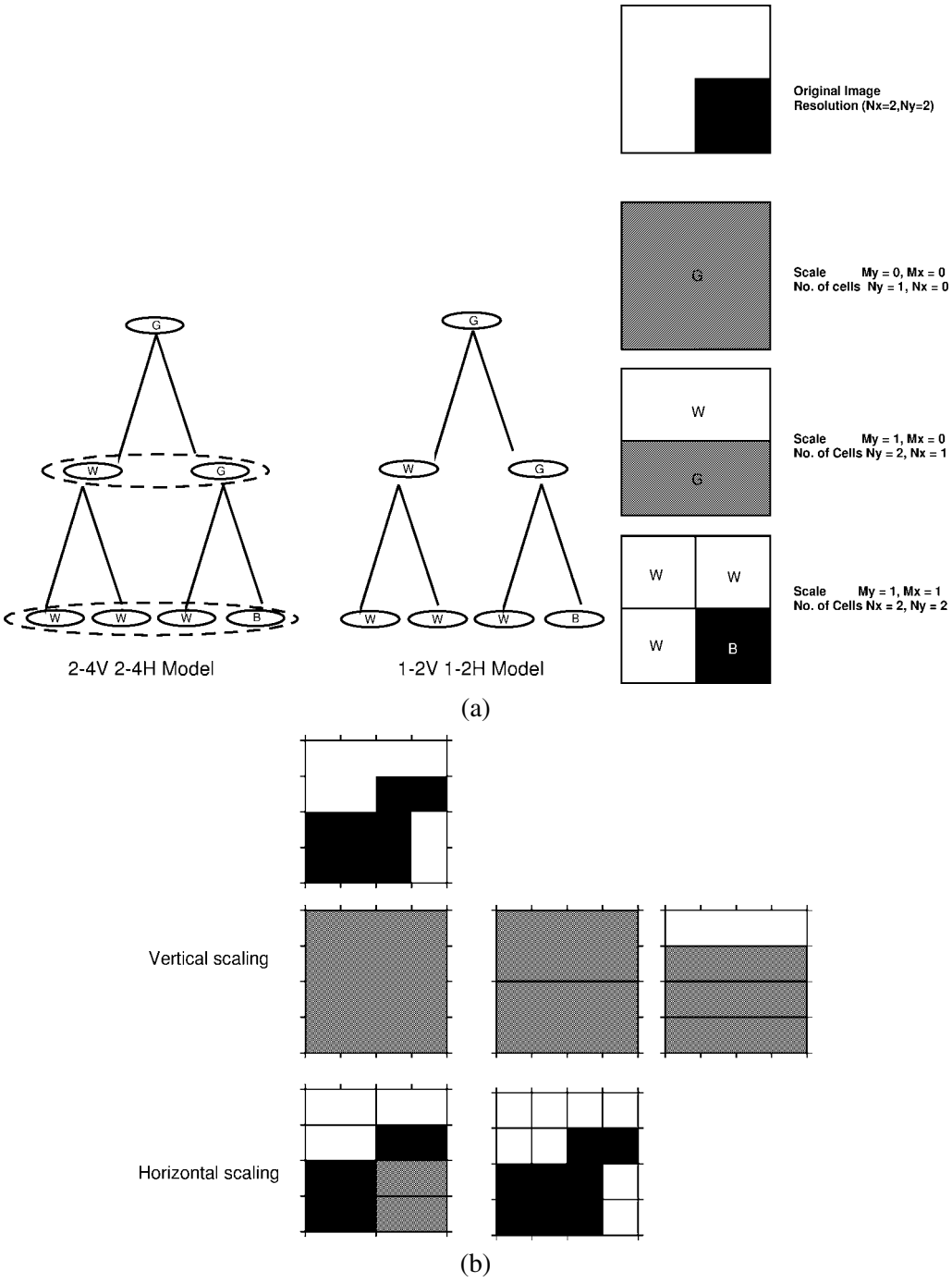

Figure 3. Dyadic tree representation of an image. (a) The sketch is the tree description of an image: right side is the image decomposition and the two left trees show two different tree representations. (b) The sketch shows an image and the steps in its scale resolution.

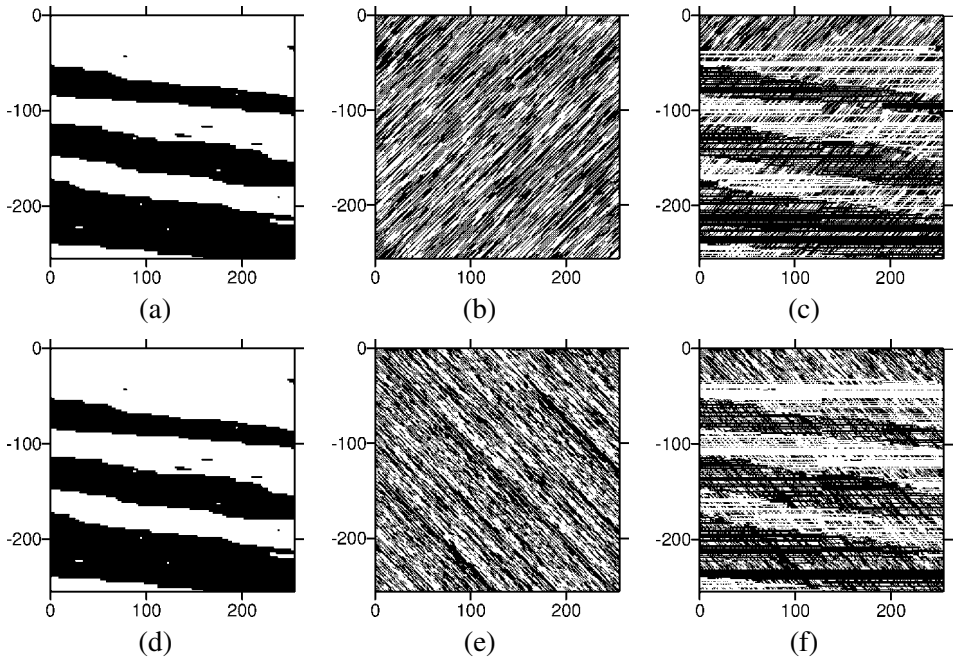

Figure 4. Merging large-scale stratification with small-scale cross-bedding at 45 ((a)–(c)) and at 135 degrees ((d)–(f)). (a), (b), (d), (e) are the input synthetic data and (c), (f) are output simulation, image resolution 256×256.

simulation procedure we also consider the 2-4V 2-4H model. In this model one considers the joint distribution of the two fathers having the same father and the corresponding four children (see figure 3(a), left).

Some numerical simulations with the dyadic tree are performed. In the first example we merge large-scale stratification with cross-bedding at 45 and 135 degrees, respectively. Figures 4(a), (b), (d), (e) are the synthetic data for this example. It is assumed that both black and white layers in the large-scale structure contain the same bedding characteristics, which is in reality not necessarily the case. The simulation result in figures 4(c), (d) shows embedding of the cross-bedding structure in the large-scale stratification.

In the second example we merge stationary data having an identical anisotropic spatial structure with other data having a different correlation structure. In this example, the method shows many applications. For instance, it can be used to simulate stationary fields. If the input data contains two realizations of stationary fields (see figures 5(a) and (b)) the simulation result will also be a stationary field (see figure 5(c)). This example illustrates the generality of our technique, which is capable of addressing stationary and non-stationary data. In the bottom row of figure 5 we show how different heterogeneity features at very close scales can be merged together to produce compound heterogeneity. In this example the data are two stationary random fields with differ-

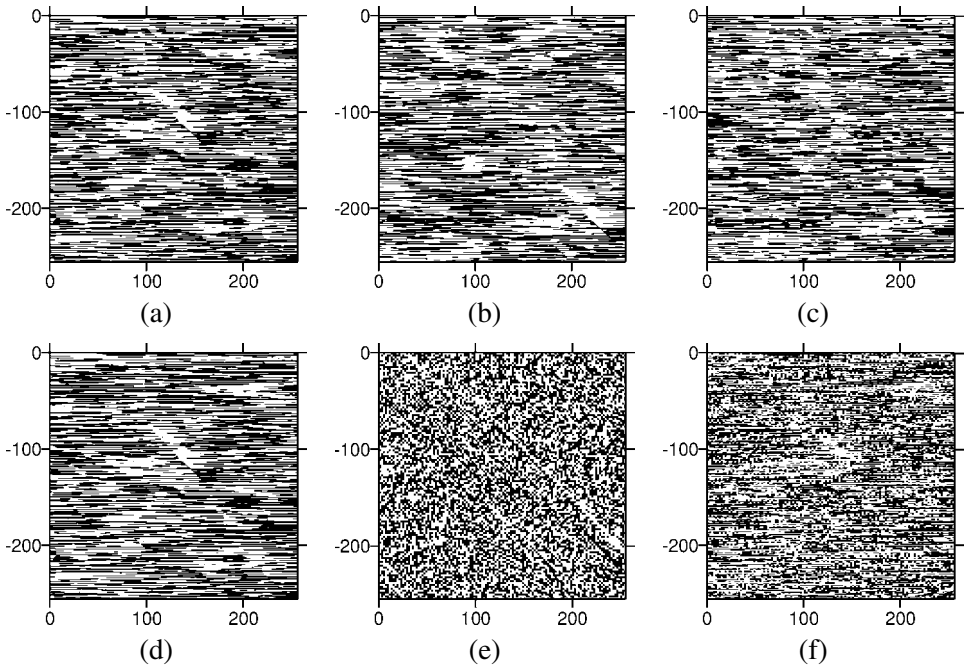

Figure 5. Merging stationary fields with identical anisotropic spatial structures to produce stationary random fields (left two columns are the input synthetic data and right shows the output realizations, image resolution 256×256).

ent correlation structures. The image of figure 5(d) is an anisotropic correlated field while the image of (e) is an isotropic random field. The simulation results of merging these two different fields produce compound fields that are displayed in figure 5(f). This example could also be used to generate complex pore structures for pore-network models.

3.4. Polychromatic trees

All the previous simulations deal with back and white images (binary images). However, the technique is more general. One can relax the assumption that each stratigraphic layer has the same fine-scale structure (as in figures 2 and 4). We illustrate this with an example.

The data for this example, presented in figure 6, would be considered as a large-scale structure stratigraphic sequence that is known with certainty (figures 6(a), (b)) while the fine-scale structure that is embedded in that structure is uncertain. This is a realistic geological assumption. The procedure can generate realizations of both structures and preserve the deterministic information of the large-scale structure, while it produces many possible realizations of the fine scale structure (see figures 6(c), (d)).

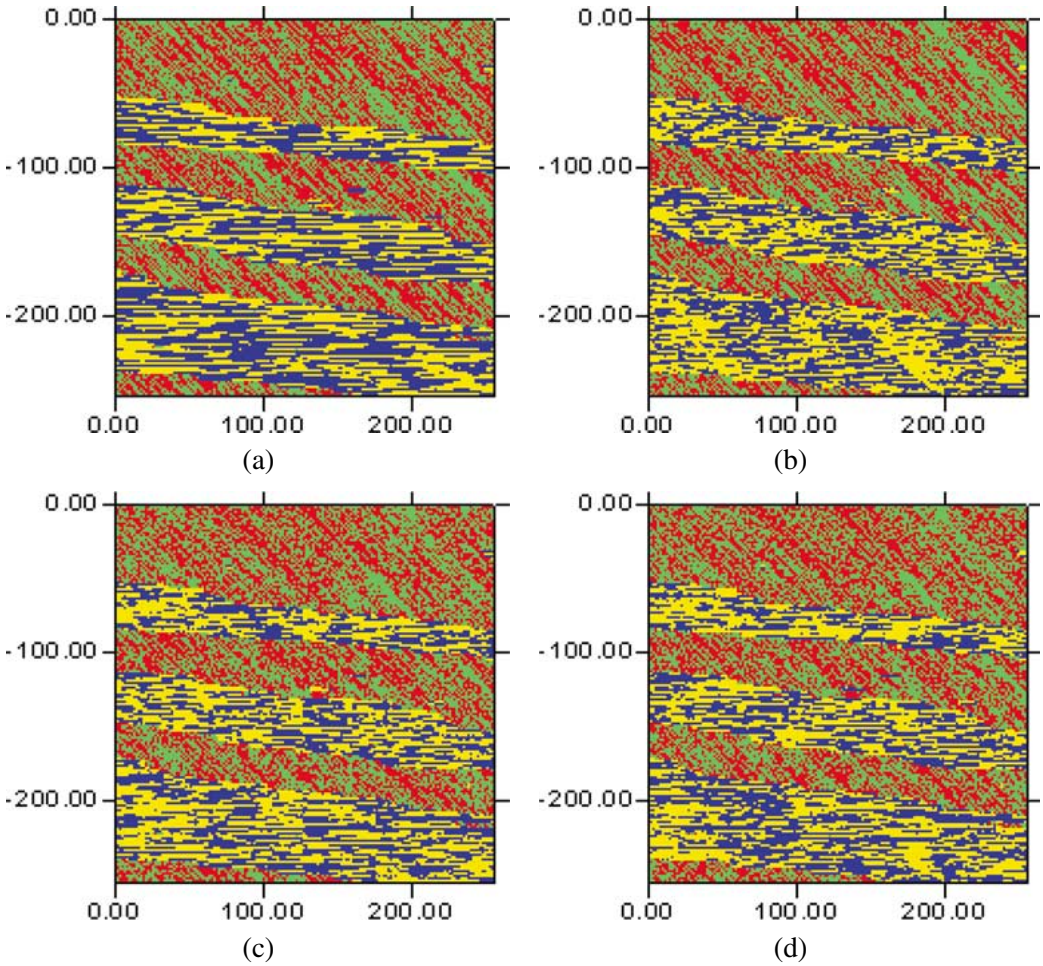

Figure 6. A heterogeneous subsurface image of two large scale structures with different fine scale structures. (a), (b): data; (c), (d): simulations.

4. Conclusions

A statistical framework for characterizing multi-scale heterogeneous structures has been developed. The framework is based on hierarchical representation of images. Although powerful and flexible this representation has some inherent artefacts. These are caused by the regular subdivision into different scales, and the fact that the (tree) Markov property still leads to too much independence in the model. As we saw these effects may be attenuated by refining the basic model, leading to a technique which is attractive for many applications. It has been illustrated in this study how this methodology can be used for characterization of subsurface heterogeneity at multiple scales. Computer codes written in FORTRAN have been developed to implement this method. The programs are flexible and permit the user to insert his own ideas. Extensive series of numerical ex-

periments have been carried out to investigate the applicability of this new methodology to subsurface characterization. Synthetic data are generated using the coupled Markov chain model, developed in [5], which are used as input for the proposed methodology. The following conclusions can be drawn from the performed experiments:

1. The proposed methodology is capable of merging different heterogeneity patterns at various scales. This is often encountered in geological data in a form of horizontal laminations or cross bedding with large-scale stratigraphic layers.
2. Fractures at various angles, stationary fields, nested and compound structures can be addressed.
3. The methodology is flexible in the sense that one can adjust input data to match well-described field settings.
4. Conditional simulation is inherent in the technique: it does not require any special procedures. Features provided by the data that are positioned in the same location in the data set (i.e., well logs, large-scale seismic information) will be *exactly* reproduced in the simulations.
5. One of the advantages of the proposed methodology among many other methods is that the uncertainty in the simulations will be bounded by the ranges provided by the data, i.e., there are no outliers in the marginals of the generated realizations.
6. The highly detailed geological structures resulting from this methodology can be utilized for further simulation modeling of the dynamic behavior of the reservoir. It provides the ability to study the influence of the microscale heterogeneity on the large-scale predictions of flow and transport in porous media. This point has been partly investigated and some results are presented in [8].

Acknowledgements

This study is financially supported by the DIOC project "Observation of the Shallow Subsurface", Delft University of Technology, Delft, The Netherlands.

References

[1] J. Bruining, D. van Batenburg, L.W. Lake and An Ping Yang, Flexible spectral methods for the generation of random fields with power-law semivariograms, Math. Geology 29 (1997) 823–848.
[2] G.R. Cross and A.K. Jain, Markov random field texture models, IEEE Trans. Pattern Anal. Mach. Intelligence 5(1) (1983).
[3] F.M. Dekking, C. Kraaikamp and J.G. Schouten, Binary images and inhomogeneous tree-indexed Markov chains, Rev. Roumaine Math. Pures Appl. 44 (1999) 181–188.
[4] C. Deutsch and A. Journel, *GSLIB: Geostatistical Software Library and User's Guide* (Oxford Univ. Press, New York, 1992).
[5] A.M.M. Elfeki, *Stochastic Characterization of Geological Heterogeneity and Its Impact on Groundwater Contaminant Transport*, Ph.D. thesis, Delft University of Technology (A.A. Balkema Publishers, Rotterdam, The Netherlands, 1996).

[6] A.M.M. Elfeki, A hybrid stochastic model for characterisation of subsurface heterogeneity, Mansoura Univ. Engrg. J. 22(3) (1997).
[7] A.M.M. Elfeki and F.M. Dekking, A Markov chain model for subsurface characterization: Theory and applications, to appear in Math. Geology (2001).
[8] A.M.M. Elfeki, F.M. Dekking, J. Bruining and C. Kraaikamp, Influence of the fine scale heterogeneity patterns on large scale behavior of miscible transport in porous media, in: *7th European Conf. on Mathematics of Oil Recovery*, EAGE, Baveno, Italy, 25 1–7.
[9] A.M.M. Elfeki, G.J.M. Uffink and F.B.J. Barends, Stochastic simulation of heterogeneous geological formations using soft information, with an application to groundwater, in: *Groundwater Quality: Remediation and Protection, QG'95*, eds. K. Kovar and Krasny, IAHS Publication 225 (1995).
[10] A.M.M. Elfeki, G.J.M. Uffink and F.B.J. Barends, A coupled Markov chain model for quantification of uncertainty in transport in heterogeneous formations, in: *GeoENV'98, 2nd European Conf. on Geostatistics for Environmental Applications*, Valencia, Spain, eds. A. Soares and J. Hernandez (Kluwer Academic, Dordrecht, 1998).
[11] H. Haldorsen and E. Damsleth, Stochastic modelling. J. Petroleum Technology 42(4) (1990) 127–139.
[12] R.W.D. Killy and G.L. Moltyaner, Twin lake tracer test: Methods and permeabilities, Water Resources Res. 24(10) (1988) 1585–1613.
[13] S.P. Neuman, in: *Recent Trends in Hydrogeology*, ed. T.N. Narasimhan, Spec. Pap. Geol. Soc. Amer. 189 (Boulder, Colorado, 1980) 81–102.
[14] H. Samet, *Applications of Spatial Data Structures* (Addison-Wesely, Reading, MA, 1990).
[15] J.L. van Beek and E.A. Koster, Fluvial and estuarine sediments exposed along the Oude Maas (The Netherlands), Sedimentology 19 (1972) 237–256.
[16] E. Vanmarcke, *Random Fields: Analysis and Synthesis* (MIT Press, Cambridge, MA, 1983).
[17] K.J. Weber, How heterogeneity affects oil recovery, in: *Resevoir Characterization*, eds. L.W. Lake and H.G. Carroll, Jr. (Academic Press, New York, 1986) 487–544.
[18] J. Yarus and R. Chambers, *Stochastic Modeling and Geostatistics Principle, Methods and Case Studies*, AAPG Computer Applications in Geology 3 (Amer. Assoc. Petroleum Geologists, 1994).